THE JOURNAL OF PHYSICAL CHEMISTRY B

Article

pubs.acs.org/JPCB

Transient Step-Like Kinetics of Enzyme Reaction on Fragmented-Condensed Substrates

Elena Del Favero,[†] Antonio Raudino,[‡] Martina Pannuzzo,[‡] Paola Brocca,[†] Simona Motta,[†] and Laura Cantú*,[†]

[†]Department of Medical Chemistry, Biochemistry and Biotechnologies, University of Milan, L.I.T.A., Via F.lli Cervi 93, 20090 Segrate, Italy

[‡]Department of Chemical Science, University of Catania, Viale A. Doria 6, 95125, Catania, Italy

Supporting Information

ABSTRACT: We followed the process of enzymatic digestion of ganglioside GD1a, operated by sialidase on aggregated micelles. The product is the ganglioside GM1, lacking the external sialic acid. The structural aspects and the kinetics connected to the process occurring on a fragmented-condensed substrate, the ganglioside micelles, are investigated by small angle X-ray scattering (SAXS). Observed at short times, the kinetics of the reaction shows a transient step-like decay, while it tends to a smooth Michaelis–Menten kinetics in the late stages. We propose a model, based on the fragmented-condensed nature of the substrate, that well reproduces the experimental observation without invoking any feedback mechanism in the reaction, usually required for an oscillatory behavior. The model predicts an initial regime dominated by the strict enzyme–substrate interaction, with a step-like appearance.

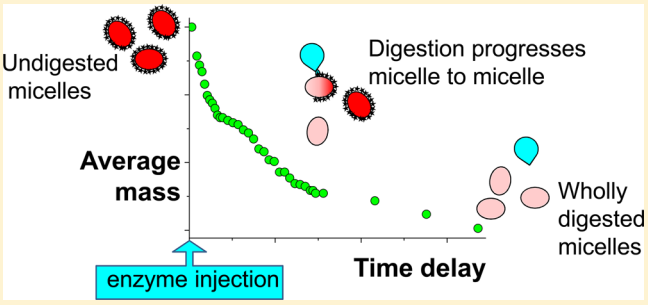

1. INTRODUCTION

A single enzyme, single substrate Michaelis–Menten (MM) reaction mechanism has demonstrated both weakly damped oscillations (stable spiral) and sustained oscillations (limit cycle) when the reaction mechanism is coupled to other biochemical pathways.[1] Damped oscillations have also been generated in open reactions by coupling very simple mechanisms, such as competitive inhibition of a single enzyme.[2] In both cases, a feedback mechanism among different kinetics pathways occurs, being the key prerequisite to develop an oscillatory behavior.

In this work, we show experimental evidence that, when the substrate is finely fragmented into mesoscopic phase-separated patterns (e.g., micelles), the overall degradation kinetics by a bound enzyme may develop transient step-like decay, tending to a smooth MM-type kinetics in the late stages. We propose a model that well reproduces the observed behavior based on the colloidal nature of the substrate, without invoking any feedback mechanism.

The experimental system consists of ganglioside GD1a micelles, the fragmented substrate, and sialidase, the enzyme that cuts the external sialic acid from the GD1a six-sugars headgroup,[3] transforming it into ganglioside GM1, bearing a five-sugars headgroup. In Figure 1, the chemical structure of the two gangliosides is shown. Although in dynamical equilibrium with monomers in solution, ganglioside micelles are extremely stable for hours. Typical times for ganglioside monomer exchange are very long, as commonly found for double-tail biological amphiphiles. This was experimentally shown[4] and is of course expected, due to their very low cmc ($\sim 10^{-8}$ M).[5] The fragmented-condensed character of the investigated system is shown in the cartoon of Figure 2. In Figure 2b, a group of nearest neighbors globular micelles is drawn, while, in Figure 2a, the sequence of digestion events on a single micelle is shown. The enzyme releases terminally positioned sialic acids from ganglioside headgroups. When all of the anchoring external sialic groups of one micelle have been cut, the enzyme is able to migrate to another micelle. The enlarged section of the micellar surface detailed in Figure 2a, specifies the three successive steps of the hydrolytic process on the fragmented phase:

(1) Enzyme adhesion: The enzyme is adsorbed on the micelle (fragmented phase) surface by weak unspecific interactions and specific recognition between the enzyme active cleft and the hydrolyzable sialic unit of GD1a.

(2) Enzyme translocation: The sialic acid is caught inside the catalytic pocket, hydrolyzed, and then released into the surrounding aqueous medium. The enzyme still remains bound to the micellar surface because of unspecific forces. During that time, it easily meets and binds another nearby (condensed) GD1a headgroup belonging to the same micelle.

Received: January 27, 2012
Revised: July 12, 2012
Published: July 18, 2012

   dx.doi.org/10.1021/jp303643u | J. Phys. Chem. B 2012, 116, 9570–9579

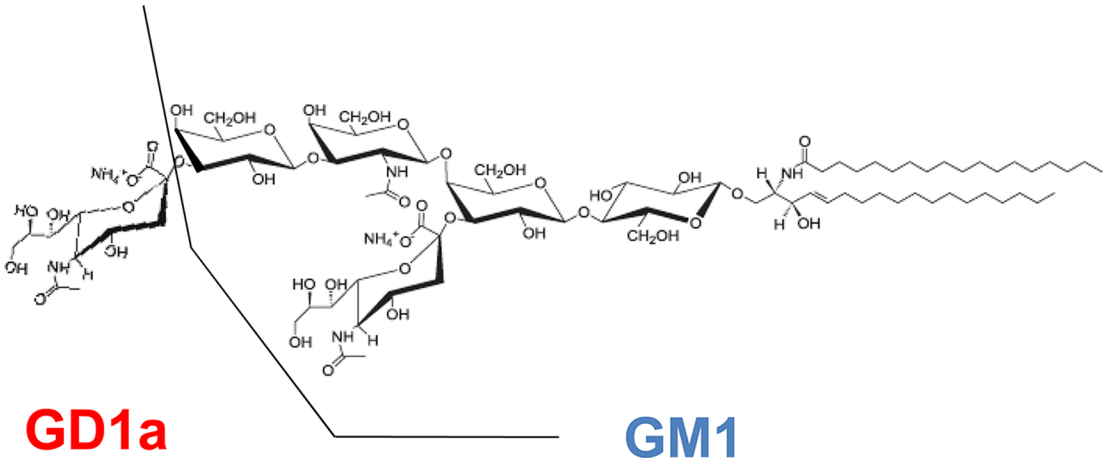

Figure 1. Chemical structure of ganglioside GD1a (PM = 1836 Da, V_{mol} = 2.356 nm^3) and of GM1 (PM = 1561 Da, V_{mol} = 2.066 nm^3).

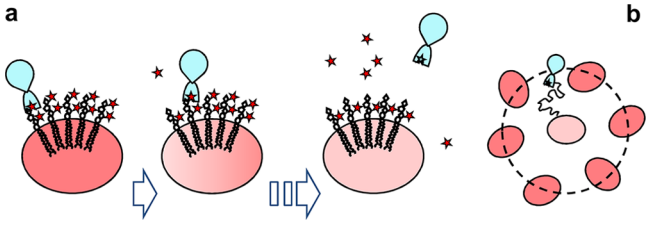

Figure 2. Pictorial sketch of enzyme hydrolysis of sialic acid from GD1a polar heads. (a) Enzyme adhesion, translocation, and release. The substrate is densely packed on the single-micelle surface but fragmented in different micelles. (b) Schematic drawing of the hydrolytic enzyme while translocating by Brownian motion from the central to a nearby micelle, located in the first solvation shell.

(3) Enzyme release: Once all of the GD1a headgroups belonging to the micelle have been hydrolyzed, unspecific forces are no longer able to catch the enzyme. Then, it escapes from the hydrolyzed micellar surface after a short residence time proportional to the strength of weak unspecific forces. The released enzyme diffuses to another micelle, where the three steps of fragmented-substrate digestion take place.

(4) From this scheme, it appears that the single-fragment (micelle) digestion occurs on the same times, irrespective of the overall stage of the reaction, while the diffusion time between a just-digested fragment to a not-yet-digested other one increases as the process goes on. Two limiting regimes are then likely to occur: the initial one, where the strict enzyme−substrate interaction dominates, and the long-time one, where diffusion processes dominate.

Our theoretical approach is based on a careful analysis of the averaging mechanisms upon which the simple MM-type theories are grounded. The dispersion of the aggregates is taken into proper account, evidencing that enzyme uptake and release are not concomitant processes in the time course of the reaction. We underline that the fragmented-condensed character is of course shared by all amphiphilic substrates, at concentrations higher than the cmc. Meanwhile, a pronounced time-stability of the aggregated structures is not at all exotic among double-tail lipids. For example, this last feature constitutes the founding concept of all of the lipid-monolayer literature, based on the Langmuir−Blodgett film experimental technique.

The output of this work points at two targets. On one hand, we show that, at variance of the oscillatory models so far presented in the literature, requiring a feedback mechanism, the widely occurring substrate fragmentation in condensed regions is itself enough to give rise to a step-like reaction, at least at the initial stages. On the other hand, this observation is of biochemical relevance in connection to the existence of membrane microdomains or rafts where substrate molecules may be preferentially segregated. Gangliosides are of such molecules.[6,7] Being in this fragmented-condensed configuration, their local concentration is much higher than average on the short length-scale, and much lower than average on the long length-scale. One can imagine that, this way, an enhanced enzyme−substrate recycle on a single microdomain (short-time) is gained at the expense of the diffusion-limited enzyme−substrate match (long-time).

We expect that peculiarities in the fragmented-condensed substrate digestion are especially relevant in the early stages of the enzyme reactions, tending to the stationary MM picture after a transient state.

2. MATERIALS AND METHODS

2.1. Experimental Section. Ganglioside GD1a, prepared as sodium salt, was extracted, purified, and chemically characterized as described in refs 8 and 9.

Sialidase was expressed in *Escherichia coli* strain called DH5α and used after purification. Zeta-potential measurements show that it carries a weak net negative surface charge (ZP ∼ −30 mV). The biochemical activity of this enzyme is to release the α-glycosidically linked and terminally positioned sialic acid (NeuAc) from sialosyl-glycoconjugates.[3,10] In our experiment, it transforms GD1a in GM1. The chemical structure of the two molecules is shown in Figure 1.

When dissolved in aqueous solution, gangliosides self-aggregate in partially dissociated micelles (∼20% of the structural charge[5]). In the very dilute regime, electrostatic interactions can be suppressed by increasing the ionic strength of the solution.[11] GD1a was dissolved in 0.1 M NaCl aqueous solution to a final concentration of 2.6×10^{-3} M (5 mg/mL) to obtain globular micelles. GD1a micellar parameters were carefully determined in the past by scattering techniques, and are reported in the literature:[12] aggregation number N = 226, hydrodynamic radius 5.8 nm, polydispersity 5%, axial ratio 0.56. The molar concentration of micelles is then 11×10^{-6} M. We note that the used GD1a concentration is orders of magnitude higher than the cmc (∼10^{-8} M).[5]

dx.doi.org/10.1021/jp303643u | J. Phys. Chem. B 2012, 116, 9570−9579

Sialidase biochemical activity on micellar systems was assessed by TLC, carried out on silica gel HPTLC plates following standard procedures.[13,14] Quantification of the ganglioside spots was performed with a Biorad 700 imaging densitometer. Figure 3 reports an example of the biochemical activity results, as a function of incubation time, as assessed by TLC.

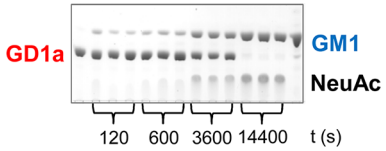

Figure 3. TLC assay on ganglioside micelles (1 mM) as a function of sialidase incubation time, namely, 2 min, 10 min, 1 h, and 4 h after enzyme addition. Assays are made in triplicate. Standard GD1a (starting molecule) and GM1 (final molecule) are reported in the first and last lanes, respectively, for ganglioside identification in the vertical direction. Progressive formation of free NeuAc is visible in the third lower row.

The structural evolution of micelles undergoing the sialidase digestion process was followed by small angle X-ray scattering (SAXS). Samples were put into polycarbonate capillaries (ENKI, Italy), 2 mm internal diameter. SAXS experiments were performed at the ESRF high-brilliance synchrotron facility (Grenoble, FR) on the ID02 beamline, in the range of momentum transfer q = 0.15−3 nm^{-1} (wavelength of the incident beam λ = 0.1 nm). Several frequent frames, with very short measurement time (0.1 s), were acquired to follow the kinetics of the system. The intensity $I(q)$ scattered by the micellar system, as a function of the momentum transfer q, was obtained after careful subtraction of empty cell and solvent contributions. Figure 4a shows some spectra collected online on ganglioside micelles while undergoing the sialidase action. Only few spectra are shown in the figure, for clarity. From top (GD1a micelles) to bottom (fully digested GD1a micelles), measurements were taken at different delays from sialidase direct addition in the measurement cell, from few seconds to hours, until complete digestion. The bottom spectrum has been collected at 36 h delay.

As interparticle interactions are negligible, due to the low concentration of micelles and the presence of added 0.1 M NaCl,[15] $I(q)$ is connected to the dimension and shape of the particles and to their contrast profile[16]

$$I(q) = \alpha \cdot \sum_n (C_n \cdot M_n^2 \cdot P_n(q, \Delta\rho_n))$$

where α is an instrumental constant and C_n is the number concentration of micelles with molecular weight M_n and form factor $P(q, \Delta\rho n)$.[17] $\Delta\rho_n$ is the contrast profile term. For $q \to 0$, the scattered intensity is simply

$$I(0) = \alpha \cdot \sum_n (C_n \cdot M_n^2 \cdot \langle \Delta\rho_n \rangle^2)$$

where $\langle \Delta\rho_n \rangle$ is the average contrast term of the n-type particle. For X-rays, it corresponds to the electron density difference between the micelle and the solvent occupying the same volume, a very high difference in the case of sugar-containing molecules. In Figure 1, some molecular parameters for GD1a and GM1 are reported. It can be seen that the removal of one sugar from the ganglioside headgroup operated by sialidase

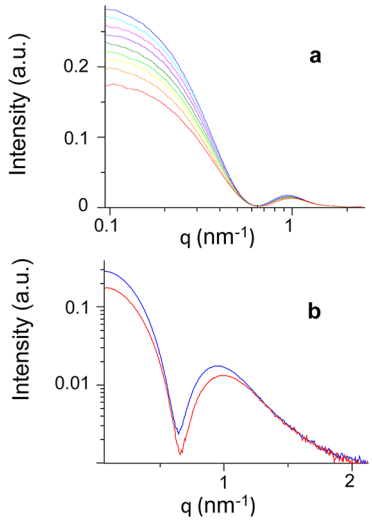

Figure 4. (a) Online evolution of SAXS spectra (top to bottom) of GD1a micelles (concentration of monomers: c = 2.6 mM (5 mg/mL); concentration of micelles: C_M^o = 11.5 × 10^{-6} M; solvent: 100 mM NaCl) after the addition of sialidase at different delays (for graphical clarity, only a selection of spectra is reported in log−lin scale): the intensity at low q progressively decreases. (b) SAXS spectra before (blue line) and after (red line) enzyme action (lin−log scale): also, the position of the minimum slightly shifts to higher q. Chemically, the starting system is GD1a and the final is GM1. Complete fits of the two micellar form factors are reported in Supporting Information A.

sensibly reduces the molecular mass of each monomer (−17%), giving great visibility to the evolution of the system along the enzymatic reaction by SAXS. To follow the kinetics of the process, the extrapolated values of $I(0)$ were recovered from each of the experimental spectra and plotted (Figure 5) as a

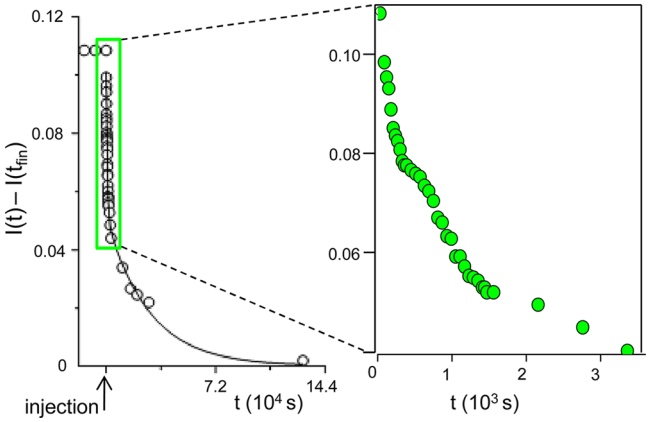

Figure 5. Time evolution of the extrapolated scattered intensity $I(q \to 0)$ of GD1a micelles as a function of sialidase incubation time. On the left side, the long-time kinetics (36 h) is shown. The arrow indicates enzyme injection and the full line corresponds to a double exponential fit, as described in the text. The short-time (1 h) behavior is enlarged on the right side of the figure, showing a step-like evolution. By that time, 1 h, roughly 60% of the initial scattered intensity has been lost.

function of time, from seconds to hours. While holding in general terms whatever the concentration, nonetheless an optimal molar ratio between enzyme and substrate has to be chosen, in order to track the structural evolution of micelles by scattering techniques. On one hand, the concentration of micelles cannot be too low. In fact, variations of the scattered

dx.doi.org/10.1021/jp303643u | J. Phys. Chem. B 2012, 116, 9570−9579

intensity on short time-delays have to be detected, with good signal-to-noise ratios. On the other hand, digestion has to be slow enough that the connected structural evolution is detectable on the same time scale. In principle, an additional caution should be considered, that is, the biochemical-digestion time scale has to be short in order to decouple it from an eventual "colloidal" rearrangement, corresponding to a change in the monomer hindrance, occurring, if present, on longer times.[18] This rearrangement has been shown not to occur in this case.[19] On a trial-and-error basis, the optimal enzyme:micelle mole ratio of the order of 1:10 was selected.

2.2. Theoretical Model: General Outline. Consider a hydrolysis process described by a chain of consecutive reactions:

$$M_N + E \rightarrow M_N^* \tag{1}$$

$$M_N^* \rightarrow M_{N-1}^* + P \tag{2a}$$

$$M_{N-1}^* \rightarrow M_{N-2}^* + P \tag{2b}$$

....

$$M_n^* \rightarrow M_{n-1}^* + P \tag{2n}$$

....

The first equation (1) describes the binding of an enzyme E onto a micelle M_N with aggregation number N (the micelle−enzyme complex is denoted M_N^*). As visually sketched in Figure 2, the bound enzyme sequentially hydrolyzes the micelle heads, releasing products P into the surrounding aqueous medium. Consequently, the number of nonhydrolyzed heads decreases from M_N^* to M_n^* (with $0 < n < N$). We specify that, unless in very diluted micellar solutions, the micelle−enzyme binding process is faster than the *full* micelle hydrolysis, whence an equilibrium between bound and free enzymes is rapidly attained (see Supporting Information D). This assumption does not mean at all that the hydrolysis of each monomer is slow. It merely states that the time required to fully hydrolyze the micelle heads is longer, due to the large aggregation number of the investigated micelles ($N \sim 200$).

It is most useful to introduce the concept of *turnover cycle*. The first cycle defines the time required to fully hydrolyze a given population of enzyme−micelle complexes obtained after a fast equilibration of a first set of enzymes and micelles in rapid equilibrium in solution. Similarly, the second cycle defines the time required to hydrolyze a new population of complexes formed when the enzymes, released from fully hydrolyzed micelles belonging to the first population, *infect* again the surrounding micelles. Identical reasoning holds for what concerns the third, fourth, and so on turnover cycles.

Let $C_n(j, t)$ be the probability of having at time t a micelle that contains n nonhydrolyzed heads in a generic jth turnover cycle. The kinetic equations associated to the scheme $(1 - 2n)$ read

$$\frac{dC_N(j, t)}{dt} = -k_N C_N(j, t) \tag{3a}$$

....

$$\frac{dC_n(j, t)}{dt} = -k_n C_n(j, t) + k_{n+1} C_{n+1}(j, t) \qquad n < N \tag{3n}$$

....

$$\frac{dC_o(j, t)}{dt} = k_1 C_1(j, t) \tag{4}$$

with k_n being a measure of the kinetics efficiency. The above equations, describing the digestion process within the *individual jth turnover cycle*, must satisfy obvious initial conditions: $C_N(j, t)|_{t=0} = \bar{C}(j)$, where $\bar{C}(j)$ is the concentration of infected micelles, and $C_n(j, t)|_{t=0} = 0$ when $n < N$, that is, at the beginning of a jth turnover cycle ($t = 0$), all of the infected micelles ($\bar{C}(j)$) carry all N nonhydrolyzed heads.

Next, we make three useful assumptions:

(a) We assume that only a single enzyme is adsorbed onto the micelle surface, where it remains bound until the micelle hydrolysis has gone to completion. Thus, the bound enzyme concentration onto a single micelle is $C_E^{Bound} = 1/N$; that is, it depends on the substrate size.

(b) For the reasons discussed in the Introduction, we neglected the effect of monomer exchange between water and micelle. However, even in the presence of a significant exchange rate, the validity of the model is preserved. Indeed, monomer exchange merely rescales the effective aggregation number N entering in the kinetic equations that being always greater than the geometrical one.

(c) In most chain reactions similar to those described by (3), like the radical depolymerization (unzipping) kinetics of polymer chains,[20] the transition probability k_n is held constant. Here k_n depends on the encounter probability among nonhydrolyzed heads on the infected micelle and the bound enzyme. k_n must decrease as the number n of nonhydrolyzed heads decreases:

$$k_n \approx k(n/N)C_E^{Bound} \approx k(n/N^2)$$

Letting $\bar{C}(1)$ be the equilibrium concentration of *infected* micelles in the first turnover cycle and making use of the mass conservation law, referred to the total available concentration of micelles, $C_M^\circ = C_M + \bar{C}(1)$, and of enzyme, $C_E^\circ = C_E + \bar{C}(1)$, the condition for the chemical reaction E + M = EM to be in equilibrium implies that

$$\frac{(C_E^\circ - \bar{C}(1))(C_M^\circ - \bar{C}(1))}{\bar{C}(1)} = \frac{1}{K_{eq}} \tag{5}$$

with K_{eq} being the equilibrium constant for the micelle−enzyme complex. Solving (4) for $\bar{C}(1)$

$$\bar{C}(1) = \frac{1}{2}(K_{eq}^{-1} + C_M^\circ + C_E^\circ - \sqrt{(K_{eq}^{-1} + C_M^\circ + C_E^\circ)^2 - 4C_M^\circ C_E^\circ}) \tag{6}$$

the above procedure, employed to calculate the equilibrium concentration $\bar{C}(1)$ of *infected* micelles in the first turnover cycle, can be extended to calculate the concentrations in all the cycles following the first one. Since after the first cycle the number of available nonhydrolyzed micelles is smaller, the equilibrium concentration of *infected* micelles in the second cycle is still calculated by (6), where we replaced the amount C_M° of available micelles by those surviving after the first cycle, $C_M^\circ - \bar{C}(1)$. Namely,

$$\bar{C}(2) \equiv \frac{1}{2}(K_{eq}^{-1} + C_M^\circ - \bar{C}(1) + C_E^\circ - \sqrt{(K_{eq}^{-1} + C_M^\circ - \bar{C}(1) + C_E^\circ)^2 - 4(C_M^\circ - \bar{C}(1))C_E^\circ}) \equiv f(\bar{C}(1)) \tag{7}$$

dx.doi.org/10.1021/jp303643u | J. Phys. Chem. B 2012, 116, 9570−9579

Analogously,

$$\bar{C}(3) = f(\bar{C}(2) + \bar{C}(1))$$

$$\bar{C}(4) = f(\bar{C}(3) + \bar{C}(2) + \bar{C}(1))$$

....

$$\bar{C}(j) = f\left(\sum_{j'=1}^{j} \bar{C}(j' - 1)\right) \tag{8}$$

(see Supporting Information B to view the behavior of the concentration of micelle−enzyme complexes, $\bar{C}(j)$ (j = 1, ..., 4) as a function of the initial micelle and enzyme concentrations, C_M° and C_E°).

2.2.1. Early Stage of the Kinetics (First Hydrolysis Cycle j = 1). Let us focus on the first hydrolysis cycle where no micelles have been still fully hydrolyzed and therefore the enzyme release is extremely unlikely. Within the above approximations, we rewrite the kinetics equations (3, 4) as

$$\frac{dC_N(1, t)}{dt} = -\kappa N C_N(1, t) \tag{9a}$$

$$\frac{dC_n(1, t)}{dt} = \kappa[-nC_n(1, t) + (n + 1)C_{n+1}(1, t)]$$

$$n < N \tag{9n}$$

$$\frac{dC_o(1, t)}{dt} = \kappa C_1(1, t) \tag{10}$$

with $\kappa \equiv k/N^2$. Similar differential-difference equations describe *pure death* processes and are well-known in the literature. They appear in the theory of stochastic processes[21] and queuing models[22] and have wide applications in many ecological[23] and financial problems.[24] Imposing the boundary condition that, at the beginning of the first turnover cycle (t = 0) all of the infected micelles ($\bar{C}(1)$) carry all N nonhydrolyzed heads, $C_N(1, t)|_{t=0} = \bar{C}(1)$, eq 8a can be solved giving

$$C_N(1, t) = \bar{C}(1)e^{-\kappa N t} \tag{11}$$

A successive substitutions−eliminations procedure, shown in Supporting Information C, yields an exact analytical solution for the concentrations $C_n(1, t)$

$$C_n(1, t) = \bar{C}(1)\binom{N}{n}\exp(-n\kappa t)(1 - \exp(-\kappa t))^{N-n} \tag{12}$$

Relevant parameters can be obtained from (12). Let us assume that the release of the enzyme occurs only when the last hydrolyzable sialic group anchoring the enzyme to the micelle surface has been cut off, as sketched in Figure 2. It follows that the flux of leaving enzymes, $J_E^{free}(1, t) \equiv dC_E^{free}/dt$, is equal to the formation rate of fully hydrolyzed micelles, $dC_o(1, t)/dt$, given by (9)

$$J_E^{free}(1, t) = \frac{dC_o(1, t)}{dt} = \kappa C_1(1, t) \tag{13}$$

Using the explicit expression for $C_1(1, t)$, eq 12, eventually we find

$$J_E^{free}(1, t) = \kappa \bar{C}(1) N \exp(-\kappa t)(1 - \exp(-\kappa t))^{N-1} \tag{14}$$

where $\kappa \equiv k/N^2$. The plot of the enzyme release rate distribution (14) against t for the first hydrolysis cycle shows that the release is basically zero at small t, it reaches a maximum at $t_{max} = N^2 \log N/k$, and then it reduces to zero at longer times. We may identify the maximum probability of the release, t_{max}, as the mean residence time of the enzyme onto the micelle surface, because at times either shorter or longer than t_{max} there is not significant enzyme release. Since the distribution (13) is not exactly symmetrical about t_{max}, a better measure of the residence time is the first moment $\langle t\rangle_{j=1}$ of the distribution function (14) that describes the averaged time the enzyme spends on the micelle surface. The normalized first moment takes the usual form: $\langle t\rangle_{j=1} = (\int_0^\infty J_E^{free}(1, t)\, dt)^{-1} \int_0^\infty t J_E^{free}(1, t)\, dt$), from which we derive a simple result

$$\langle t\rangle_{j=1} = \frac{N^2 H_N}{k} \approx \frac{N^2(\gamma + \log N)}{k} \tag{15}$$

H_N being the Nth harmonic number:[25] $H_N \equiv \sum_{k=1}^{N} (1/k) \approx \log N + \gamma + (1/2N) + O(N^{-2})$, with γ = 0.5772... the Euler's constant. Since $\langle t\rangle_{j=1} \approx t_{max}$, the two above definitions of the mean residence time do not appreciably differ.

In a similar way, we calculated the spreading of the residence time about its mean value $\langle t\rangle_{j=1}$. From the definition of variance $\sigma_E^2(1)$ (j = 1 stands for the first turnover cycle), we write the relationship

$$\sigma_E^2(1) = \left(\int_0^\infty J_E^{free}(1, t)\, dt\right)^{-1} \int_0^\infty (t - \langle t\rangle_{j=1})^2 J_E^{free}(1, t)\, dt$$

$$= \langle t^2\rangle_{j=1} - \langle t\rangle_{j=1}^2$$

that, after integration, gives another simple result

$$\sigma_E^2(1) = \frac{N^4}{k^2}\left[\frac{\pi^2}{6} - \psi'(N + 1)\right] \approx \frac{\pi^2}{6}\frac{N^4}{k^2} \tag{16}$$

where $\psi'(N + 1) \approx (1/N) + O(N^{-2})$ is the first derivative of the digamma function.[25]

Equation 16 describes the spreading of the enzyme release time when the micelle hydrolysis has gone to completion. This result, together with the one obtained for the residence time $\langle t\rangle_{j=1}$, eq 15, provides the key ingredients to simulate the overall kinetics. The dependence of $\langle t\rangle_{j=1}$ and $\sigma_E^2(1)$ on k and N will be discussed in section 3.2.1.

2.2.2. Intermediate Stage of the Kinetics (j ≥ 2). Let us now turn to the following turnover cycles. Once the bound enzyme has been released from the surface of fully hydrolyzed micelles, it becomes available for a further binding onto untransformed micelles. Once again, we make the useful assumption that the *infection* rate is much faster than the hydrolysis rate of a single micelle (an assumption guaranteed by the large aggregation number N, see Supporting Information D). We proceed in calculating the kinetics of the turnover cycles beyond the first. Naively, one might guess identical kinetics in all the cycles. A deeper analysis proves this conjecture to be wrong because of the following: (a) According to eqs 6−8, the number of *infected* micelles at the beginning of the second turnover cycle is smaller than that of the first cycle, even in an excess of substrate. This is a simple thermodynamic effect related to the concentration decrease of untransformed micelles. (b) The spreading of the enzyme residence time at the end of the first turnover cycle is large. For the same reason, the enzyme residence time at the end of the second cycle exhibits an even broader distribution. Identical considerations apply to all the following jth cycles.

The calculation of the global kinetics is not an easy matter. However, under the hypothesis of a fast enzyme migration (see Supporting Information D for justification), the *infection* rate in

dx.doi.org/10.1021/jp303643u | J. Phys. Chem. B 2012, 116, 9570−9579

the second turnover cycle, $J_E^{Bound}(2, t)$, is proportional to the enzyme release rate in the first cycle

$$J_E^{Bound}(2, t) \approx \psi_2 J_E^{free}(1, t) \tag{17}$$

with ψ_2 being a normalization factor to be determined. Equation 17 highlights the different behavior of the next turnover cycles ($j \geq 2$). Indeed, in the first turnover cycle, $j = 1$, we have a single exponential decay for the probability of finding an undigested micelle: $C_N(1, t) = \bar{C}(1)e^{-\kappa N t}$. On the other hand, in the time course of the second cycle, the decay must be replaced by a convolution of different exponentials, beginning at different times randomly distributed around the mean release time of the enzyme from nearby micelles. In other words, $C_N(2, t)$ must depend on the past history of the micellar digestion. The distribution of the enzyme release time is given by (14) and the convolution reads

$$C_N(2, t) = \psi_2 \int_0^t J_E^{free}(1, t')e^{-\kappa N(t-t')}\, dt' \tag{18}$$

This result is strongly different from that obtained in the first hydrolysis cycle $C_N(1, t)$. The procedure outlined above to calculate $C_N(2, t)$ has been extended (see Supporting Information E for details) to calculate the concentration of partially hydrolyzed micelles $C_n(2, t)$ (n stands for the number of nonhydrolyzed heads)

$$C_n(2, t) = \kappa\psi_2 \int_0^t C_1(1, t')C_n(1, t - t')\, dt' \tag{19}$$

The still unknown normalization factor ψ_2 is obtained by imposing that the integrated flux of the leaving enzyme in the second cycle must equate its equilibrium concentration:

$$\int_0^\infty J_E^{free}(2, t)\, dt = \bar{C}(2) \tag{20}$$

Since $J_E^{free}(2, t) = \kappa C_1(2, t)$, with the aid of (19) and (20), we obtain

$$\psi_2 = \bar{C}(2)\kappa^{-2}\left(\int_0^\infty \int_0^t C_1(1, t')C_1(1, t - t')\, dt'\, dt\right)^{-1} \tag{21}$$

The above procedure has been iterated to calculate $C_n(j, t)$ in all of the following cycles ($j = 3, 4, ...$).

Proceeding as before, we calculated two basic properties: the enzyme's mean residence time $\langle t \rangle_j$ onto the micelle and the standard deviation of the residence time $\sigma_E^2(j)$ at any jth turnover cycle. Two key results are as follows: (a) the duration of the enzyme residence time behaves as $\langle t \rangle_{j+1} \approx (j + 1)\langle t \rangle_1 + O(j^2)$; (b) the spreading $\sigma_E^2(j)$ of the residence time around $\langle t \rangle_j$ sharply increases with j.

2.2.3. Late Stage of the Kinetics ($j \to \infty$). After several hydrolysis cycles, the system loses memory of its initial conditions. The release of the enzyme from the micellar surface becomes a random variable uniformly distributed over time. Under the preceding assumptions, we expect that when $j \geq 4$ the enzyme release rate reaches a stationary state. The lack of oscillations at large t (namely, large j) suggests a continuous enzyme release from fully hydrolyzed micelles to undigested ones. In the large j limit, the whole kinetics can be adequately described in the realm of the classical MM type equations where the concentration of the enzyme–micelle complexes attains a constant (or slowly time-varying) value. In other words, after a transient time, kinetics becomes roughly exponential and do not exhibit any longer the step-like behavior typical of small and intermediate times.

3. RESULTS

3.1. Experimental Results. SAXS measurements were performed on the ganglioside micelles undergoing sialidase digestion at different delay times from enzyme addition.

Figure 4b shows SAXS spectra of ganglioside micelles (initially GD1a, c = 5 mg/mL, 0.1 M NaCl, finally GM1) before sialidase addition and at the very end of enzyme action (see also the same spectra in log–log scale together with the curves corresponding to the fitting form factors and fit parameters in Supporting Information A). Spectra have been fitted with the form factor of core–shell oblate ellipsoids, that is, the geometrical shape reproducing on average the ganglioside globular micelles.[5] We emphasize that, while molecular parameters of GD1a and GM1 gangliosides have been used for the initial and final systems, respectively (see Figure 1), nonetheless the micellar aggregation number (N = 220), and correspondingly the hydrophobic core volume and shape, are unvaried. Variations occur, as expected, in the hydrophilic shell thickness and hydration, both reducing, as in the final state the external and most hydrated sugars of the shell have been removed by sialidase. The overall reduction in shell thickness is of 0.3 nm. We stress that no rescaling was applied to reproduce the observed overall reduction in the scattered intensity. It can be deduced that micelles do not change their packing, although the individual monomers within the aggregates have been hugely modified in their hydrophilic moiety, both in lateral hindrance and in structural charge, being chemically turned from GD1a to GM1, as determined by TLC assay (see Figure 3). No "colloidal" modification, on the aggregate length-scale, occurs on any time-scale (even 36 h); that is, the initial micelles appear to be just mowed by the enzyme in their external sialic acid residues,[19] without changing their aggregation number.

The fact that the ganglioside micellar mass reduction occurs at constant aggregation number is an interesting finding. No structural rearrangement on the colloidal scale, driven by processes like monomer exchange, are observed, even over long times. It can be justified by considering the high hydrophobicity of gangliosides (cmc $\sim 10^{-8}$ M) and their structurally adaptive character. On one hand, the single whole-micelle digestion is much faster than the monomer exchange process. If ever, the sialic-acid removal, operated by sialidase, brings an increase in the monomer hydrophobicity, that is, in its residence time within the aggregate. Monomer exchange occurs on a one-at-a-time sporadic basis. On the other hand, once packed in the aggregate, gangliosides have shown a strongly cooperative structural behavior; that is, the collection dictates the spatial arrangement of single exchanging monomers. Then, unexpectedly but welcome, the present observations reinforce the hypothesis that the micellar aggregate constitutes a packing trap for the slow-exchanging gangliosides, as inferred from the strong hysteresis effects formerly observed.[18,26,27] For what concerns the present enzymatic digestion experiment, the extreme stability of the ganglioside packing guarantees that the extent of fragmentation of the substrate does not change during the process.

In between the two extreme stages of digestion, several spectra have been collected at different delays from enzyme addition. A selection, for clarity, is reported in Figure 4a. It can be seen that spectra progressively transform from the initial (top) to the final (bottom), reproducing the progressive

dx.doi.org/10.1021/jp303643u | J. Phys. Chem. B 2012, 116, 9570–9579

transformation of the *average micelles*. The intermediate spectra could be reproduced either by a linear combination of the extremes or by a progressive evolution of the shell thickness and hydration at constant aggregation number, and, of course, by a superposition of the two processes. An eventual increase in polydispersity, already affecting (~5%) the initial collection of micelles,[12] cannot be appreciated from the experimental data. On the contrary, the extrapolated scattered intensities at $q = 0$, $I(0)$, can be determined with confidence from the spectra and can be reported as a function of time, that is, of the delay from enzyme addition, as in Figure 5, illustrating the time evolution of the *average micelle*, as recalled in section 2.1.

Figure 5 shows the time evolution of the extrapolated scattered intensity, reduced in terms of excess with respect to the final value, $I(0, t) - I(0, t_{final})$. At t_{final}, the enzymatic digestion process has been completed and, as tested by TLC, all of the GD1a has been turned into GM1. On the left, the whole kinetics is reported, from $t = 0$ to $t_{final} = 36$ h, together with a double exponential fit ($t_1 = 780$ s, $t_2 = 28000$ s). On the right, the short-time region is enlarged, revealing an unusual step-like evolution.

The appearance of more than one decay time suggests that a transition occurs between different regimes. At short times, the kinetics of chemical digestion dominates, while the physical approach (diffusion process) dictates the long delay behavior. We recall that, by SAXS, we detect the evolution of the structural properties of micelles, that is, the final result of the enzymatic digestion, strongly affecting the monomer configuration by removing one sugar group from the headgroup. The fragmented-condensed nature of the micellar substrate is likely to enhance the discrepancy of the different regimes and, most strikingly, it is likely to be at the basis of the step-like behavior in the short-time region.

3.2. Theoretical Results. In this section, we specify the theoretical model outlined before to explicit the influence of the fragmented-condensed character of the substrate in the micellar form on the reaction kinetics at increasing delays from enzyme addition. Three different regimes are found (early, intermediate, and late stages), as outlined in section 2.2, and are summarized as follows.

3.2.1. Early Stage of the Hydrolysis Kinetics. This regime is characterized by the following:

(a) The enzyme is adsorbed onto a limited number of micelles rapidly reaching an equilibrium between free and adsorbed enzyme.

(b) At the beginning of the first turnover cycle ($t = 0$), all of the infected micelles carry all N nonhydrolyzed heads. On this basis, the kinetic equations can be exactly solved for the concentrations of partially hydrolyzed micelles $C_n(1, t)$.

(c) The release of the enzyme occurs only when all of the hydrolyzable groups of the infected micelle have been cut off, as sketched in Figure 2.

This leads to the expression reported in eq 12 for the flux of leaving enzymes, $J_E^{free}(1, t)$, showing a maximum at a certain delay t_{max} that identifies the mean residence time of the enzyme onto the micellar surface. In fact, no significant enzyme release is present at times either shorter or longer than t_{max}. More accurately, a better measure of the residence time is the first moment $\langle t \rangle_{j=1}$ that in the large N limit is

$$\langle t \rangle_{j=1} \approx \frac{N^2 \log N}{k} \tag{22a}$$

and the spreading of the residence time about its mean value $\langle t \rangle_{j=1}$, when the micelle hydrolysis has gone to completion, is indicated by the variance (see also eq 16)

$$\sigma_E^2(1) \approx \frac{\pi^2}{6}\frac{N^4}{k^2} \tag{22b}$$

As already noted, eqs 22a and 22b provide the key ingredients to simulate the overall kinetics. As we can see, the mean residence time of the enzyme, eq 22a, increases with the micelle's aggregation number N and decreases with the hydrolysis rate constant k. In the fast adsorption limit, the initial distribution of bound enzyme is a narrow, almost impulsive, function of time. On the contrary, the enzyme release, that occurs when the last anchoring lipid head that has been cut off, is broadly distributed over time (see eq 22b). The dependence of the dispersion $\sigma_E^2(1)$ on k and N is qualitatively similar to that shown by the residence time $\langle t \rangle_{j=1}$.

3.2.2. Intermediate Stage of the Hydrolysis Kinetics ($j \geq 2$). This regime occurs once the bound enzyme has been released from the surface of a "first" fully hydrolyzed micelle and it becomes available for a further binding onto a "second" undigested micelle, then "third" and following. It still holds that the *infection* rate is much faster than the hydrolysis rate of a single micelle, thanks to the large aggregation number N.

However, a careful analysis shows that the hydrolysis rate in the second turnover cycle differs from that calculated in the first cycle. Indeed: (a) The number of *infected* micelles at the beginning of the second turnover cycle is smaller than that of the first cycle, even in excess substrate conditions. This is a thermodynamic effect related to the decrease of the concentration of undigested micelles. (b) The spreading of the enzyme residence time in the second turnover cycle is broader than that observed during the first cycle, a general property of the conditional probability. Identical considerations apply to all the following cycles $j > 2$.

The detailed calculation of the global kinetics has been developed in section 2.2. Under the hypothesis of a fast enzyme migration, the *infection* rate in the second turnover cycle, $J_E^{Bound}(2, t)$, is proportional to the enzyme release rate in the first cycle: $J_E^{Bound}(2, t) \approx \psi_2 J_E^{free}(1, t)$, with ψ_2 being a normalization factor. In the second hydrolysis cycle, the decay must be replaced by a convolution of different exponentials, each of them beginning at a different time conditioned by the distribution of the enzyme release time from nearby micelles. This process is described by a convolution integral. It means that the hydrolysis in the second cycle does strictly depend on the kinetics of the first cycle (see eq 19).

The procedure outlined above has been extended (see section 2.2 for details) to obtain the concentration of partially hydrolyzed micelles $C_n(j, t)$ in subsequent cycles of the intermediate regime (n stands for the number of nonhydrolyzed heads, and j, an integer, denotes the hydrolysis cycle).

Proceeding as before, the enzyme's mean residence time $\langle t \rangle_j$ onto the micelle surface and the standard deviation of the residence time $\sigma_E^2(j)$ for any jth turnover cycle can be derived.

Two results are worth mentioning: (a) the duration of the enzyme residence time roughly behaves as $\langle t \rangle_{j+1} \approx (j + 1)\langle t \rangle_1 +$ *small j-dependent terms*; (b) the spreading $\sigma_E^2(j)$ of the residences time around $\langle t \rangle_j$ sharply increases with j.

Numerical results are shown in Figure 6, where we report the release rate of the free enzyme against the elapsed time t. At $t = 0$, the enzyme is added to the suspension and most of it rapidly

dx.doi.org/10.1021/jp303643u | J. Phys. Chem. B 2012, 116, 9570−9579

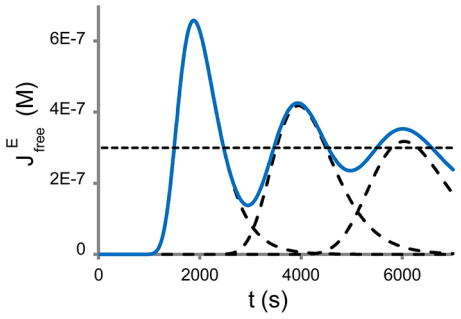

Figure 6. Enzyme release rate $J^E_{free}(t)$ against the elapsed time for an enzyme-containing micellar solution. The dashed curves describe the rate for each turnover cycle, and the full line is the total effect calculated by adding together the dashed curves. At $t = 0$, we impose a prescribed concentration $\bar{C}(1) = 1.1 \times 10^{-6}$ M of enzyme−micelle complexes. Notice that at large t the rate $J^E_{free}(t)$ asymptotically approaches a constant value.

binds to the micelle surface, so the release rate is extremely small. At $t = \langle t \rangle_1$, the hydrolysis of the *infected* micelles has gone to completion and the enzyme is released in the bulk solution, giving rise to a burst of free enzyme concentration near $t = \langle t \rangle_1$ (the first peak in Figure 6). The freed enzyme is then adsorbed by nearby intact micelles, shifting again the release rate toward lower values. Oscillations self-replicate in the following turnover cycles. Uptake kinetics behaves analogously, and at long times, it is identical to the release rate. Enzyme release and uptake times, however, rapidly broaden with the number of cycles, dampening the calculated oscillatory behavior until a stationary value of free enzyme concentration in the bulk is attained after a few cycles. In other words, the system progressively loses memory of its initial state in the following enzyme release−uptake processes.

3.2.3. Late Stage of the Hydrolysis Kinetics ($j \to \infty$). This regime occurs after several hydrolysis cycles, when the system loses memory of its initial conditions. The release of the enzyme from the micellar surface becomes a random variable uniformly distributed over time, reaching a stationary state. Under the preceding assumptions, we expect this to occur when $j \geq 4$, as evidenced in Figure 6. The lack of oscillations at large t (namely, at large j, late cycles) suggests a continuous release of enzyme from fully hydrolyzed micelles to unmodified ones. The concentration of the enzyme−micelle complexes attains a constant value. The whole kinetics can be adequately described with a classical MM type exponential equation and does not exhibit any longer the step-like behavior calculated in the preceding regimes. In this late limit, smearing hinders the peculiar phenomenology connected to the fragmented-condensed nature of the substrate, as observed on the macroscopic scale, merging in an "average" behavior.

3.3. Building of the Expected Experimental Behavior.

The step-like kinetics described so far reveals the importance of the condensed-dispersed nature of the substrate in the timing of enzyme action. It is likely to be effective whenever the substrate is locally tightly packed in dispersed clusters, either in solution, like micelles, or on a supporting matrix, like a membrane. Despite its putatively wide field of application, its experimental observation is easily hindered by averaging or limited by experimental sensitivity. A more accessible, but strictly related, variable is the total amount of products freed in the time course of the hydrolysis. In the present case, the total amount of hydrolyzed sialic groups released in the bulk solution could be measured, or the digested lipid, for example, by TLC assay, as shown in Figure 3. We have instead employed the SAXS technique, measuring the evolution of the scattered intensity of a micellar suspension due to the enzyme hydrolysis of the ganglioside head groups, as shown in the Experimental Section. Together with the whole spectrum, the extrapolated value of the scattered intensity at $q \to 0$ can be evaluated. On the other hand, the expected extrapolated scattered intensity at different delays, $I(t)$, referred to in the preceding section, can be reconstructed on the basis of the proposed model in the following way.

The decrease of the intensity $I(t)$ upon enzyme addition at $t = 0$ is a nonlinear function of the hydrolysis degree. It is easy to show that we may partition the total intensity as

$$I(t) = I_1(t) + I_2(t) \tag{23}$$

where the first contribution, $I_1(t)$, comes out from the untransformed micelles, while $I_2(t)$ describes the scattering intensity of fully and partially transformed micelles. Specifically,

$$I_1(t) \approx \alpha \cdot (C^\circ_M - \sum_{j'=1}^{j} \sum_{n=1}^{N} C_n(j', t)) \cdot (\Delta\rho_{in})^2 M_{in}{}^2 \tag{24}$$

where α is an instrumental constant, $C^\circ_M - \sum_{j'=1}^{j} \sum_{n=1}^{N} C_n(j', t)$ is the concentration of the undigested micelles (in stands for initial) after j successive turnover cycles, $\Delta\rho_{in}$ is the contrast term of the undigested micelle, and M_{in} is the micellar mass. Analogously, assuming that the aggregation number N does not appreciably change in the time course of the hydrolysis (an assumption fully verified by our experimental results), the contribution $I_2(t)$ coming from fully and partially hydrolyzed micelles turns out to be

$$I_2(j, t) \approx \alpha \cdot \sum_{j'=1}^{j} \sum_{n=1}^{N} C_n(j', t) \left[\frac{N-n}{N} \Delta\rho_{fin} + \frac{n}{N} \Delta\rho_{in} \right]^2 \times \left(\frac{n}{N} M_{fin} + \frac{N-n}{N} M_{in} \right)^2 \tag{25}$$

where $\Delta\rho_{fin}$ and M_{fin} (fin stands for final) are the associated micelle contrast and mass, respectively, $C_n(j, t)$ is the concentration of micelles with n nonhydrolyzed heads in a generic jth turnover cycle, and the other symbols have been previously defined. The sum of the two contributions described above reproduces the time evolution of the scattered intensity. It is convenient to introduce a dimensionless relative intensity defined as

$$I_{rel}(t) = \frac{I(t) - I_{fin}}{I_{in} - I_{fin}} \tag{26}$$

with I_{in} and I_{fin} being the intensities of the nonhydrolyzed and fully hydrolyzed micellar suspensions, respectively. $I_{rel}(t)$ varies from 1 to 0, and it is independent of the instrumental constant α.

In Figure 7, we plot the reconstructed total scattering intensity versus the time elapsed from enzyme addition, following the theoretical model. As expected, the damped oscillations of the enzyme release rate described in Figure 6 introduce some steps in the micellar hydrolysis kinetics. Steps appear in the early stages of the hydrolysis and are expected to rapidly vanish with time. Furthermore, provided the other parameters are kept constant, the length of each step is expected to be very sensitive to the micelle aggregation number

dx.doi.org/10.1021/jp303643u | J. Phys. Chem. B 2012, 116, 9570−9579

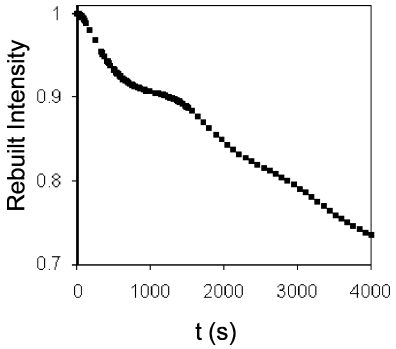

Figure 7. Theoretical rebuilding of the expected relative scattered intensity at $q \to 0$, $I_{rel}(t) = (I(t) - I_{fin})/(I_{in} - I_{fin})$, as a function of the delay time from enzyme addition, on the basis of the proposed model. Steps are expected to appear at short times and to smear progressively.

N (roughly as $N^2 \log N$), while the height of the steps slightly decreases with N. Lastly, it is worth mentioning that the general topology of the reconstructed curves remains almost unchanged on varying both enzyme and substrate concentrations (data not shown).

4. DISCUSSION

In this work, we consider the enzymatic digestion of a substrate that is condensed on the local scale but fragmented in mesoscopic clusters, namely, GD1a ganglioside micelles. Following the scheme of Figure 2, it appears that two events are to be considered:

(a) *The single micelle digestion.* This process is expected to occur on the same times irrespective of the overall stage of the reaction, provided that the enzyme is kept on the individual infected micelle until all of its monomers have been digested. This hypothesis is reasonable, as on the micelle the substrate is condensed, so that the probability to shift to a neighboring monomer on the same micelle is much higher than that to diffuse to another micelle. We notice that both the sialidase enzyme and the ganglioside micelle are negatively charged, so that short-range attractive interactions must exist, more than compensating electrostatic repulsion until the substrate is digested.

(b) *The migration of the enzyme from one digested micelle to a suitable other.* At the beginning of the reaction, this process is very rapid as compared to fragment digestion. This is the model assumption, based on the high number of enzyme−monomer interactions occurring before the enzyme leaves the micelle, corresponding to the high aggregation number, ∼200, of the micelle. Then, due to the fragmented-condensed nature of the system, enzyme uptake and release are not concomitant processes in the time course of the reaction. With this sole assumption, the experimentally observed step-like behavior is well reproduced. The migration process, of course, becomes slower as the reaction proceeds. In fact, while the overall number of micelles, and then the probability of enzyme−micelle match, remains unchanged, the number of suitable (undigested) micelles decreases. The number of useless enzyme−micelle matches increases in time.

As described in the preceding sections, two limiting regimes are then expected. In the initial one (early + intermediate stages in the model), the strict enzyme−substrate interaction dominates and the migration time between fragments is negligible. As far as the extent of fragmentation is concerned, under the assumption that the other parameters keep constant values, the model predicts a $N^2 \log N$ dependence for the length of the steps (see section 3.2.1). In the final regime (late stage in the model), the diffusion process dominates and a longer time is spent by the enzyme to find a substrate.

A transition should exist between the very early stage, when the simultaneity of enzyme assault is preserved, and an intermediate stage when smearing occurs. According to the model, the dispersion σ should depend on the fourth power of the aggregation number, N^4, then, lower for smaller micelles.

Looking at Figures 5 and 7, the agreement between experiment and theoretical prediction is easily seen. Nonetheless, an interesting discrepancy can be observed. In the experiment, the individual steps seem to increase in length as the digestion process proceeds (Figure 5). At present, this fact is not deeply treated in the proposed model, as the step-like behavior, corresponding to the highly concomitant assault of micelles, is expected to be rapidly washed out by dispersion in the enzyme release from different micelles. As shown in Figure 6, enzyme-release events are expected to occur at almost constant delays, over the first few cycles. The wash-out time (after which the MM picture is attained) is expected to be shorter than the time required for slowing down the "useful" diffusion to match the single-fragment digestion. Of course, the time-mismatch depends on the concentrations of micelles and enzymes, both absolute and relative. In the experiment, the step-like behavior is seen to persist longer than predicted. This discrepancy could be related to a small but non-negligible contribution of the monomer exchange rate between water and micelles, an effect not considered in our model. As said in section 2.2, the inclusion of the monomer exchange merely rescales the effective aggregation number N entering in the kinetic equations that becomes greater than the geometrical one. Other explanations, however, are possible. The permanence of the step-like behavior, indicating a long-lived simultaneity of enzyme assault, could be connected to some peculiar trajectory of the enzyme on the micelle surface, for example, moving along a percolation line rather than randomly jumping from one digested ganglioside headgroup to an undigested one.

5. CONCLUSION

We followed the process of enzymatic digestion of a condensed-fragmented substrate, namely, the action of sialidase on the headgroup of ganglioside GD1a, aggregated in micelles. The nanodispersed colloidal nature of the micellar substrate gives rise, at short times, to a transient pronounced step-like behavior of the enzyme kinetics. Only at later stages, this unusual feature washes out to merge in the usual smooth Michaelis−Menten kinetics. We show that this interesting behavior can be theoretically well reproduced by just focusing on the fragmented-condensed nature of the substrate, without invoking any feedback mechanism in the reaction, usually required for an oscillatory behavior. This case is likely to be of general biochemical relevance, as enzyme action in biological systems is commonly operated on nonbulk substrates. It reveals the importance of the condensed-dispersed nature of the substrate in the timing of enzyme action. It can happen whenever the substrate is locally tightly packed in dispersed clusters, either in solution, like micelles, or on a supporting matrix, like a membrane. Moreover, we refer to the sialidase−ganglioside enzyme−substrate pair, an intriguing case in connection to the existence of membrane microdomains where gangliosides are known to be preferentially segregated.

dx.doi.org/10.1021/jp303643u | J. Phys. Chem. B 2012, 116, 9570−9579

■ ASSOCIATED CONTENT

Supporting Information

Supporting Information A: Fits of micellar form factors. Supporting Information B: Concentration of micelle−enzyme complexes. Supporting Information C: Concentration of partially hydrolyzed micelles in the first cycle. Supporting Information D: Enzyme binding kinetics. Supporting Information E: Concentration of partially hydrolyzed micelles in all turnover cycles. This material is available free of charge via the Internet at http://pubs.acs.org.

■ AUTHOR INFORMATION

Corresponding Author

*Phone: +39 02 503 30 362. Fax: +39 02 503 30 365. E-mail: laura.cantu@unimi.it.

Notes

The authors declare no competing financial interest.

■ ACKNOWLEDGMENTS

We thank T. Narayanan for his precious assistance at the ID02 beamline. We thank S. Sonnino for kindly supplying the sialidase enzyme. We thank S. Perego for the TLC assays.

■ REFERENCES

(1) Ryde-Pettersson, U. *Acta Chem. Scand.* **1992**, *46*, 406−408.
(2) Ngo, L. G.; Roussel, M. R. *Eur. J. Biochem.* **1997**, *245*, 182−190.
(3) Tringali, C.; Papini, N.; Fusi, P.; Croci, G.; Borsani, G.; Preti, A.; Tortora, P.; Tettamanti, G.; Venerando, B.; Monti, E. *J. Biol. Chem.* **2004**, *279*, 3169−3179.
(4) Cantú, L.; Corti, M.; Salina, P. *J. Phys. Chem.* **1991**, *95*, 5981−83.
(5) Sonnino, S.; Cantú, L.; Corti, M.; Acquotti, D.; Venerando, B. *Chem. Phys. Lipids* **1994**, *71*, 21−45.
(6) Regina Todeschini, A.; Hakomori, S. I. *Biochim. Biophys. Acta* **2008**, *1780*, 421−33.
(7) Gupta, G.; Surolia, A. *FEBS Lett.* **2010**, *584*, 1634−1641.
(8) Sonnino, S.; Cantú, L.; Acquotti, D.; Corti, M.; Tettamanti, G. *Chem. Phys. Lipids* **1990**, *52*, 231−241.
(9) Tettamanti, G.; Bonali, F.; Marchesini, S.; Zambotti, V. *Biochim. Biophys. Acta* **1973**, *296*, 160−170.
(10) Monti, E.; Bonten, E.; D'Azzo, A.; Bresciani, R.; Venerando, B.; Borsani, G.; Schauer, R.; Tettamanti, G. *Adv. Carbohydr. Chem. Biochem.* **2010**, *64*, 403−79.
(11) Degiorgio, V.; Cantú, L.; Corti, M.; Piazza, R.; Rennie, A. *Colloids Surf.* **1989**, *38*, 169−178.
(12) Cantú, L.; Corti, M.; Sonnino, S.; Tettamanti, G. *Chem. Phys. Lipids* **1986**, *41*, 315−328.
(13) Chigorno, V.; Tettamanti, G.; Sonnino, S. *J. Biol. Chem.* **1996**, *271*, 21738−44.
(14) Mauri, L.; Casellato, R.; Kirschner, G.; Sonnino, S. *Glycoconjugate J.* **1999**, *16*, 197−203.
(15) Cantú, L.; Corti, M.; Degiorgio, V.; Piazza, R.; Rennie, A. *Prog. Colloid Polym. Sci.* **1988**, *76*, 216−220.
(16) Lindner, P.; Zemb, T. *Neutron, X-rays and Light: Scattering Methods Applied to Soft Condensed Matter*; Elsevier (North-Holland Delta Series): Amsterdam, The Netherlands, 2002.
(17) Pedersen, J. S.; Svaneborg, C. *Curr. Opin. Colloid Interface Sci.* **2002**, *7*, 158−166.
(18) Cantú, L.; Corti, M.; Del Favero, E.; Digirolamo, E.; Sonnino, S.; Tettamanti, G. *Chem. Phys. Lipids* **1996**, *79*, 137−145.
(19) Del Favero, E.; Brocca, P.; Motta, S.; Rondelli, V.; Sonnino, S.; Cantú, L. *J. Neurochem.* **2011**, *116*, 833−839.
(20) Yashin, V. V.; Isayev, A. I. *J. Polym. Sci., Part B: Polym. Phys.* **2003**, *41*, 965−982.
(21) Ross, S. M. *Introduction to probability models*; Academic Press: New York, 2007.
(22) Stewart, W. J. *Probability, Markov chains, queues, and simulation*; Princeton University Press: Princeton, NJ, 2009.
(23) Gillman, M. *An introduction to mathematical models in ecology and evolution: time and space*; Wiley-Blackwell: Hoboken, NJ, 2009.
(24) Aoki, M. Yoshikawa, H. *Reconstructing macroeconomics: a perspective from statistical physics and combinatorial stochastic processes*; Cambridge University Press: Cambridge, U.K., 2007.
(25) Abramowitz, M.; Stegun, I. A. *Handbook of Mathematical Functions*; Dover: New York, 1972.
(26) Boretta, M.; Cantú, L.; Corti, M.; Del Favero, E. *Physica A* **1997**, *236*, 162−176.
(27) Cantú, L.; Corti, M.; Del Favero, E.; Digirolamo, E.; Raudino, A. *J. Phys. (Paris)* **1996**, *6*, 1067−1090.